Large Molecule Therapeutics

Preclinical Activity of the Type II CD20 Antibody GA101 (Obinutuzumab) Compared with Rituximab and Ofatumumab *In Vitro* and in Xenograft Models

Sylvia Herter[1], Frank Herting[2], Olaf Mundigl[3], Inja Waldhauer[1], Tina Weinzierl[1], Tanja Fauti[1], Gunter Muth[2], Doris Ziegler-Landesberger[3], Erwin Van Puijenbroek[1], Sabine Lang[1], Minh Ngoc Duong[4], Lina Reslan[4], Christian A. Gerdes[1], Thomas Friess[2], Ute Baer[2], Helmut Burtscher[2], Michael Weidner[2], Charles Dumontet[4], Pablo Umana[1], Gerhard Niederfellner[2], Marina Bacac[1], and Christian Klein[1]

Abstract

We report the first preclinical *in vitro* and *in vivo* comparison of GA101 (obinutuzumab), a novel glycoengineered type II CD20 monoclonal antibody, with rituximab and ofatumumab, the two currently approved type I CD20 antibodies. The three antibodies were compared in assays measuring direct cell death (AnnexinV/PI staining and time-lapse microscopy), complement-dependent cytotoxicity (CDC), antibody-dependent cell-mediated cytotoxicity (ADCC), antibody-dependent cell-mediated phagocytosis (ADCP), and internalization. The models used for the comparison of their activity *in vivo* were SU-DHL4 and RL xenografts. GA101 was found to be superior to rituximab and ofatumumab in the induction of direct cell death (independent of mechanical manipulation required for cell aggregate disruption formed by antibody treatment), whereas it was 10 to 1,000 times less potent in mediating CDC. GA101 showed superior activity to rituximab and ofatumumab in ADCC and whole-blood B-cell depletion assays, and was comparable with these two in ADCP. GA101 also showed slower internalization rate upon binding to CD20 than rituximab and ofatumumab. *In vivo*, GA101 induced a strong antitumor effect, including complete tumor remission in the SU-DHL4 model and overall superior efficacy compared with both rituximab and ofatumumab. When rituximab-pretreated animals were used, second-line treatment with GA101 was still able to control tumor progression, whereas tumors escaped rituximab treatment. Taken together, the preclinical data show that the glyoengineered type II CD20 antibody GA101 is differentiated from the two approved type I CD20 antibodies rituximab and ofatumumab by its overall preclinical activity, further supporting its clinical investigation. *Mol Cancer Ther; 12(10); 2031–42. ©2013 AACR.*

Introduction

The CD20 monoclonal antibody (mAb) rituximab has revolutionized treatment of non-Hodgkin's lymphoma (NHL) and chronic lymphocytic leukemia (CLL) in combination with chemotherapy. However, indolent malignancies such as CLL and follicular lymphoma remain largely incurable and a significant proportion of patients with diffuse large B-cell lymphoma (DLBCL) still relapse.

Therefore, it remains a medical need for improved treatments and novel CD20 antibodies to be developed.

Obinutuzumab (GA101) is a novel type II, humanized, CD20 mAb that has been glycoengineered to reduce core fucosylation, conferring enhanced affinity for the human FcγRIIIa receptor on effector cells and, hence, enhanced antibody-dependent cell-mediated cytotoxicity (ADCC; refs. 1, 2). As a type II mAb, GA101 has lower capacity to relocalize CD20 into lipid rafts upon binding compared with type I antibodies and is a less potent in inducing complement-dependent cytotoxicity (CDC) but more potent in mediating homotypic cell adhesion and direct cell death (3, 4). Results of epitope mapping and crystallography indicate that GA101 and rituximab bind adjacent and partially overlapping epitopes on CD20 but acquire different orientation upon binding (5–7), which most likely contributes to different biologic characteristics of type I and II antibodies (6).

Ofatumumab, a type I antibody like rituximab, is approved for treatment of patients with CLL refractory to fludarabine and alemtuzumab (8, 9). In preclinical studies, ofatumumab was a more potent mediator of CDC than rituximab (10). Ofatumumab binds to a different

epitope on CD20, involving both the small and large loops of CD20 (5, 11, 12). It is not yet known whether the increased CDC activity of ofatumumab is clinically relevant as there are currently no head-to-head clinical data available.

The current study provides, for the first time, a direct comparison of preclinical activity of type II antibody GA101 with that of the type I antibodies rituximab and ofatumumab in a panel of *in vitro* and *in vivo* studies.

Materials and Methods

Reagents

GA101 and rituximab were obtained from F. Hoffmann-La Roche AG. Ofatumumab was obtained from a local pharmacy. The experimental study protocol was reviewed and approved by the Roche Group ethical committee.

Cell culture

Raji and WIL2S cells were purchased from ECACC (European Collection of Cell Cultures; Ref: 85011429 and 90112121), Z138 cells were obtained from Martin Dyer (University of Leicester, Leicester, United Kingdom; cell line not authenticated), and SU-DHL4 cells from DSMZ (Deutsche Sammlung für Mikroorganismen und Zellkulturen; Ref: ACC 495). Raji and WIL2 NS cells were cultivated in Dulbecco's modified Eagle medium (Invitrogen) containing 10% fetal calf serum (FCS; Invitrogen) and N-acetyl-L-alanyl-L-glutamine (2 mmol/L). Z138 cells and SU-DHL4 cells were cultivated in RPMI-1640 (Invitrogen) containing 10% FCS and N-acetyl-L-alanyl-L-glutamine (2 mmol/L). Cell line authentication was not conducted in-house. Raji, WIL2S, and SU-DHL4 were purchased from repositories that use short-tandem repeat PCR (STR-PCR) for authentication. All cell lines were expanded upon delivery and low-passage vials were stored in liquid nitrogen. The experiments were carried out within 8 weeks after thawing.

Fluorescence-activated cell sorting analysis

To compare the binding mode of type I and II antibodies, fluorescence-activated cell sorting (FACS)–binding curves were generated by titrating the GA101, rituximab, or ofatumumab. A total of 2×10^5 Z138 or SU-DHL4 cells per sample were incubated with mAb for 30 minutes at 4°C in a final volume of 200 μL. After washing, cells were incubated for a further 30 minutes at 4°C with a fluorescein isothiocyanate (FITC)–conjugated F(ab′)2 fragment goat anti-human immunoglobulin G (IgG) Fcγ (Jackson ImmunoResearch; #109-096-098). Dead cells were identified and excluded using propidium iodide (PI; Sigma-Aldrich; #P4864) staining. Measurements were carried out using the FACSCanto II (BD Biosciences). The average median fluorescence intensity and SDs were calculated in triplicates and plotted.

Evaluation of C1q binding

The binding of the human complement component C1q (Sigma-Aldrich; #C1740) to each mAb was assessed by

ELISA. Serial dilutions of the antibodies were immobilized on a MaxiSorp 96-well plate. Free binding sites were blocked with PBS containing 3% bovine serum albumin (Sigma-Aldrich; #A3059) followed by incubation with C1q (2.2 μg/mL) at room temperature for 90 minutes. Plates were washed and bound C1q were detected using polyclonal rabbit anti-human C1q (Dako; #A0136) with horseradish peroxidase–conjugated polyclonal goat anti-rabbit Fc (Jackson ImmunoResearch; #111-035-046) and 2,2′-azino-bis(3-ethylbenzothiazoline-6-sulfonic acid (ABTS; Roche; #11684302001). Measurements were carried out using an automated microplate reader (405 nm/490 nm).

Assessment of direct cell death, ADCC, CDC, whole-blood assay

The assays were conducted as described by Mossner and colleagues (1). A brief description is present in the Supplementary Data.

Assessment of ADCP

Monocyte-derived macrophages (MDM) were generated by plating 8×10^6 monocytes [isolated from human peripheral blood mononuclear cell (PBMC) derived from healthy blood donors] in a T75 flask and incubating for 6 to 7 days in RPMI-1640 containing FCS (10%), L-glutamine (1%), and macrophage colony-stimulating factor (M-CSF; 60 ng/mL; PeproTech; #300-25). MDMs were further polarized for 24 hours with 100 ng/mL human IFN-γ (PeproTech; #300-02) and 100 ng/mL lipopolysaccharide (LPS; Sigma-Aldrich; to generate M1 macrophages) or for 48 hours with 10 ng/mL human IL-10 (PeproTech; #200-10; to generate M2c macrophages). Both subpopulations have been characterized by cytokine release and expression of surface markers. M1 secreted IL-12, TNF-α, IP10, and IL-6, whereas M2c produced IL-10. Both subpopulations expressed CD68. Furthermore, M1 highly expressed MHC class II as well as CD80 on their surface, whereas M2c expressed CD163. CD206 was significantly stronger for M2c but was also detectable on M1 and therefore was used as FACS marker for macrophages in the antibody-dependent cell-mediated phagocytosis (ADCP) assay. For the ADCP assay, PKH26- or CFSE (Sigma-Aldrich; #PKH26-GL and #21888)–labeled Raji cells were incubated with M1 or M2c macrophages for 1 hour at 37°C [effector:target (E:T), 3:1] in the presence of different CD20 antibody concentrations, before staining with CD206-FITC and anti-CD22-APC (BioLegend; #321104 and #302510) and FACS analysis. ADCP was determined by gating PKH26$^+$/CD206$^+$/CD22$^-$ cells and analyzing the percentages of gated cells, which include phagocytosed target cells but exclude target cells only attached to the surface of the macrophages. The averages and SDs of the triplicates of each experiment were calculated. The assessment of ADCP in presence of competing endogenous human IgGs was conducted by addition of 10 mg/mL Redimune (Behring) to the assay [4 hours ADCP with human M2c macrophages and Raji (E:T 3:1) in the presence of GA101, rituximab, and ofatumumab at

1 μg/mL]. Three independent experiments were carried out.

CD20 internalization

To assess CD20 internalization after binding of antibodies, SU-DHL4 cells and fresh human blood derived from 2 patients with CLL were incubated for 0.5, 2, 4, or 7 hours (SU-DHL4) and for 0.5, 1, 2, 3, and 5 hours (primary CLL samples) with Alexa Fluor 488 (Life Technologies)–labeled GA101, rituximab, or ofatumumab (all 5 μg/mL) at 37°C. Cells were then washed and incubated in the presence or absence of quenching anti-Alexa Fluor 488 for 30 minutes at 4°C. The remaining fluorescence indicates the amount of labeled antibody that is not accessible to the quenching anti-Alexa Fluor 488 antibody and thus corresponds to internalized antibody. The average fluorescence intensity and SDs were calculated from duplicates of the experiment with SU-DHL4 cells. Because of low number of primary CLL samples, the average fluorescence intensity in B and C corresponds to single values. The amount of surface-accessible CD20 was calculated as follows:

$$\text{Percentage surface-accessible CD20}$$
$$= 100 - \frac{\text{median fluorescence quenched } \alpha\text{CD20}}{\text{median fluorescence } \alpha\text{CD20}} \times 100.$$

Live-cell imaging and confocal microscopy analysis

For direct monitoring, antibodies were directly labeled with Alexa Fluor 488 or 568 (Invitrogen). Z138 cells were seeded at 1.5×10^6/mL on poly-L-ornithine–coated glass coverslips (Lab-Tek) and incubated with 5 μg/mL of Alexa Fluor–labeled antibodies at 37°C on a microscope stage incubator, maintaining temperature and CO_2. Images were taken on a Leica TCS SP5 X confocal laser scanning microscope using white-light laser excitation at 497 and 578 nm (at $63\times$/1.2NA water immersion). Selective spectral detector emission band passes for each dye were used in sequential scanning mode. High-sensitivity, low-noise detectors (HyD) were used for image acquisition. The detection pinhole size was set to 1 Airy unit (AU); voxel size, 0.98 to 1.96 μm. For cell-death induction, Z138 cells were treated with 20 μg/mL antibody together with the Annexin V FLUOS/PI Labeling Kit (Roche). Apoptosis markers were excited at 497 and 578 nm, respectively, using white-light laser excitation in sequential scanning mode. Transmission images were recorded simultaneously. Time-lapse image series were collected every 3 minutes simultaneously for all four conditions (control/rituximab/GA101/ofatumumab) by using the multiposition feature of the Leica AF control software. During the time lapse (6 hours), cells were maintained at 37°C on a microscope stage incubator.

In vivo antitumor activity

The human DLBCL cell line SU-DHL4 was subcutaneously inoculated (5×10^6 cells) with Matrigel (BD Biosciences) into the right flank of 4- to 5-week-old female severe combined immunodeficient (SCID) beige mice (Charles River Laboratories) maintained under the standard conditions. Female SCID beige mice (Charles River Laboratories), 4 to 5 weeks of age, were maintained under specific pathogen-free conditions according to guidelines. Continuous health monitoring was carried out on a regular basis, with daily monitoring of clinical symptoms and adverse effects. Primary tumor volume (TV) was calculated according to the National Cancer Institute (NCI; Bethesda, MD) protocol [TV = (length × width^2)/2], where "length" and "width" are the long and short diameters of the tumor mass in millimeters. Antitumor activity was assessed by calculating tumor-growth inhibition (TGI) based on medians by using the following formula:

$$100 - \frac{\text{Average}[T\_\text{treatment (day } x) - T\_\text{treatment (baseline)}]}{\text{Average}[T\_\text{reference (day } x) - T\_\text{reference (baseline)}]} \times 100.$$

At 25 days after cell transplantation, 10 animals with established subcutaneous SU-DHL4 tumors (>500 mm^3) were randomized to vehicle control, single-agent GA101, rituximab, or ofatumumab [all 30 mg/kg intraperitoneally (i.p.)]. Treatment commenced 25 days after tumor-cell inoculation (median tumor volume, 504–571 mm^3), with administration repeated on days 32, 39, 46, 53, and 60. TGI was assessed on day 46 after tumor-cell inoculation, and animals were observed until day 67 to evaluate tumor status. To evaluate second-line antitumor activity, mice bearing tumors with a median volume of 504 to 571 mm^3 received rituximab (10 mg/kg, i.p.) on days 25 and 32 after tumor-cell inoculation (median tumor volume, 626–633 mm^3) and were randomized to vehicle control, single-agent GA101, rituximab, or ofatumumab (all 30 mg/kg, i.p.). Second-line treatment was administered on study days 39, 46, 53, 60, and 67, with second-line antitumor activity evaluated on day 63 after tumor-cell inoculation. The human indolent NHL cell line RL was subcutaneously inoculated (10×10^6 cells) into the right flank of the mice, and after 14 days, 10 animals with established subcutaneous RL tumors (median volume, 150 mm^3) were randomized to each group: vehicle control, single-agent GA101, rituximab, and ofatumumab (all 30 mg/kg, i.p. once-weekly over 4 weeks). TGI was assessed on day 28 after tumor-cell inoculation. Raw data from the RL experiment were processed in the statistics software SAS-JMP version 8.0.2.2 (SAS, 2007) using the menu RocheTools 3.1. Primary tumor volume and antitumor activity were calculated by using the established methods.

Results

Binding to CD20-expressing target cells

The binding of GA101, rituximab, and ofatumumab was assessed on Z138 and SU-DHL4 cell lines expressing low (60,000) and high (1,000,000) CD20 receptor copy numbers, respectively (data not shown). Despite binding to different (or partially overlapping) epitopes, GA101, rituximab, and ofatumumab competed with each other in

binding, highlighting how small the extracellular portion of CD20 is (data not shown). Titration of antibody concentrations up to 20 µg/mL showed that the maximal binding intensity of GA101 to tumor cells was approximately 50% of that observed with the same concentrations of rituximab and ofatumumab (Fig. 1A and B), consistent with previously reported data for GA101 and rituximab (1). The EC_{50} values of GA101, rituximab, and ofatumumab binding to the two NHL cell lines were comparable (0.6–1.1 µg/mL) and independent of CD20 expression level. Therefore, when bound to tumor cell lines, GA101 displayed similar EC_{50} values to the type I antibodies but occupied only half of the number of CD20-binding sites.

Redistribution of CD20 by GA101, rituximab, and ofatumumab

It has been shown that type I CD20 antibodies redistribute CD20 into Triton-insoluble membrane fractions corresponding to lipid rafts, whereas type II antibodies induce homotypic aggregation of CD20 at cell–cell contact sites (1, 5). When directly labeled antibodies were incubated with Z138 cells, we found a rapid redistribution of GA101–Alexa Fluor 568–bound CD20 complexes into homotypic adhesion sites within 30 minutes at 37°C. When rituximab–Alexa Fluor 488 was coincubated with GA101, it was excluded from the contact sites and

appeared clustered in lateral regions on the cell surface, confirming our previous observations (5). Interestingly, when ofatumumab–Alexa Fluor 488 was used in Z138 cells, the redistribution pattern was different from rituximab. Ofatumumab did not seem completely excluded from the homotypic adhesion sites. Although some sites appeared reduced in ofatumumab, others had a quite uniform localization of ofatumumab-bound CD20 complexes also in GA101-enriched clusters of CD20 (Fig. 1C). Overall, ofatumumab decorated CD20 membrane pools more uniformly when compared with rituximab. Moreover, when cells were followed over an extended period of time (>4 hours), GA101 labeling became successively attenuated, as if ofatumumab competed with GA101 for binding sites in areas of cell–cell contact (data not shown).

C1q binding and induction of CDC

The binding of the complement component C1q to the antibodies was assessed using ELISA plates coated with increasing antibody concentrations. Overall, rituximab and ofatumumab showed comparable C1q binding but bound significantly greater amounts of C1q than GA101 (Fig. 2A). The capacity to induce CDC was further compared in cellular assays using Z138 and SU-DHL4 cell lines. In accordance with C1q-binding data, GA101 displayed inferior CDC activity compared with rituximab
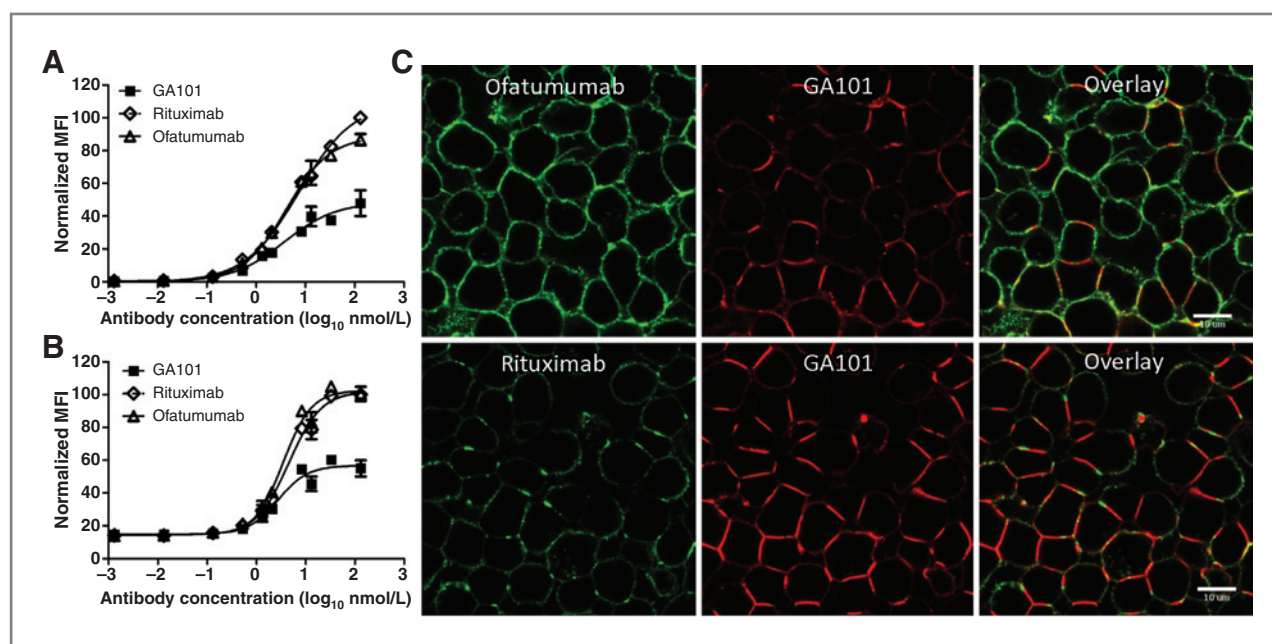

Figure 1. Antibody-binding assay comparing binding of GA101 (black squares), rituximab (open diamonds), and ofatumumab (open triangles) to CD20-expressing NHL cells Z138 (A) and SU-DHL4 (B). Cells were incubated for 30 minutes at 4°C with increasing concentrations of CD20 antibodies followed by staining using a FITC-labeled secondary antibody and flow cytometry analysis. Dead cells were excluded by PI staining. Calculated EC_{50} values using SU-DHL4: GA101, 3.7 nmol/L; rituximab, 7.4 nmol/L; ofatumumab, 4.1 nmol/L. Statistical analysis corresponding to comparison of the maximal binding on Z138 cells: GA101 versus rituximab, $P = 0.0028$; GA101 versus ofatumumab, $P = 0.0013$; rituximab versus ofatumumab, $P = 0.0006$; SUDHL4 cells: GA101 versus rituximab, $P = 0.0009$; GA101 versus ofatumumab, $P = 0.0037$; rituximab versus ofatumumab, $P = 0.9233$. C, redistribution of CD20 on Z138 cells by GA101, rituximab, and ofatumumab: top, overlay of GA101–Alexa Fluor 568- and ofatumumab-Alexa Fluor 488–bound CD20 complexes; bottom, overlay of GA101-Alexa Fluor 568–bound CD20 complexes and rituximab–Alexa Fluor 488–bound CD20 complexes. The average fluorescence intensity and SDs of one of three independent experiments were calculated from the triplicates of each experiment. MFI, mean fluorescence intensity.
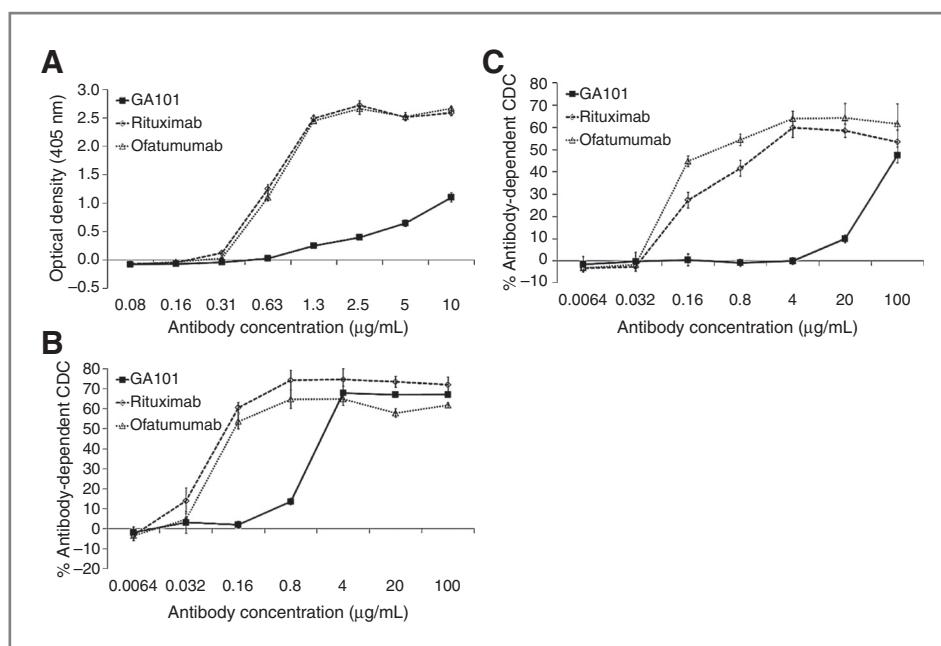
Figure 2. Binding of the complement component C1q to CD20 antibody-coated dishes (A) and CDC induced by GA101 (black squares), rituximab (open diamonds), and ofatumumab (open triangles) in two NHL cell lines, SU-DHL4 (B) and Z138 (C). Rituximab and ofatumumab bound significantly higher amounts of C1q and induced higher CDC after 2 hours of incubation with rabbit complement and different CD20 antibody concentrations. The average CDC and SDs were calculated from the triplicates of each experiment. The data from one of three independent experiments are shown. Calculated EC_{50} values for CDC with SU-DHL4: GA101, 6.3 nmol/L; rituximab, 0.42 nmol/L; ofatumumab, 0.48 nmol/L. Calculated EC_{50} values for CDC with Z138: GA101, >200 nmol/L; rituximab, 1.2 nmol/L; ofatumumab, 0.7 nmol/L.

and ofatumumab at low antibody concentrations (≤1 µg/mL for SU-DHL4 and ≤20 µg/mL Z138 cells; Fig. 2B and C), resulting in significantly inferior EC_{50} CDC values (40 µg/mL for GA101 compared with 0.17 µg/mL and 0.10 µg/mL for rituximab and ofatumumab, respectively). The inferior CDC-mediating capacity of GA101 is also reflected by the concentration required to reach the maximal CDC activity, which is more than 100 µg/mL for GA101 and is between 0.8 and 4 µg/mL for rituximab and ofatumumab on Z138 cells. The same is true for SU-DHL4 cells, on which GA101 reaches maximal CDC between 4 and 20 µg/mL, whereas rituximab and ofatumumab do so between 0.16 and 0.8 µg/mL. Notably, at high antibody concentrations (>1 µg/mL for SU-DHL4 and >20 µg/mL Z138 cells), all antibodies induced comparable levels of overall CDC. Interestingly, rituximab and ofatumumab showed comparable CDC activity in our assays using both cell lines.

Induction of direct cell death

The ability of the antibodies to induce direct cell death was assessed by detecting phosphatidylserine exposure (Annexin V FLUOS binding) and PI staining 24 hours after mAb incubation with a panel of CD20-expressing tumor cell lines. Overall, GA101 was superior to rituximab and ofatumumab in inducing cell death of Raji, WIL2S, and Z138 NHL cells (Fig. 3A). To confirm that cell-death induction by GA101 is unrelated to mechanical disruption, as recently hypothesized (13, 14), and to gain further

insights into the kinetics and mechanisms of cell death, direct cell death was assessed using time-lapse confocal microscopy and Annexin V/PI labeling of Z138 tumor cells. Figure 3B shows representative images taken at the indicated time points (cf. Supplementary Video S1). Within 1.5 hours, clear signs of Annexin V positivity, as early hallmark of cell-death induction, were detected in cells incubated with GA101, whereas the cell-death induction observed with rituximab or ofatumumab was virtually indistinguishable from that of control. After 5 hours, GA101 caused strong cell death as visualized by PI labeling of lysed cells (Fig. 3B, i–vi). Control-, rituximab-, or ofatumumab-treated cultures displayed only a slight increase in PI-positive cells. Taken together, live-cell imaging of tumor cells revealed that GA101 was faster than, and superior to, rituximab and ofatumumab in inducing direct cell death.

ADCC

The ability of GA101 [glycoengineered and wild-type (WT) antibody variants], rituximab, and ofatumumab to mediate ADCC was assessed using Z138 and SU-DHL4 target cell lines and human PBMCs expressing the V158/V158 or the F158/F158 FcγRIIIa receptor. Overall, the potency of GA101 was higher than that of rituximab and ofatumumab in both cell lines with PBMCs expressing either V158/V158 or F158/F158 FcγRIIIa receptor (Fig. 4A–D). The superiority of GA101 was apparent in terms of both EC_{50} values of target cell killing (~2 ng/mL for
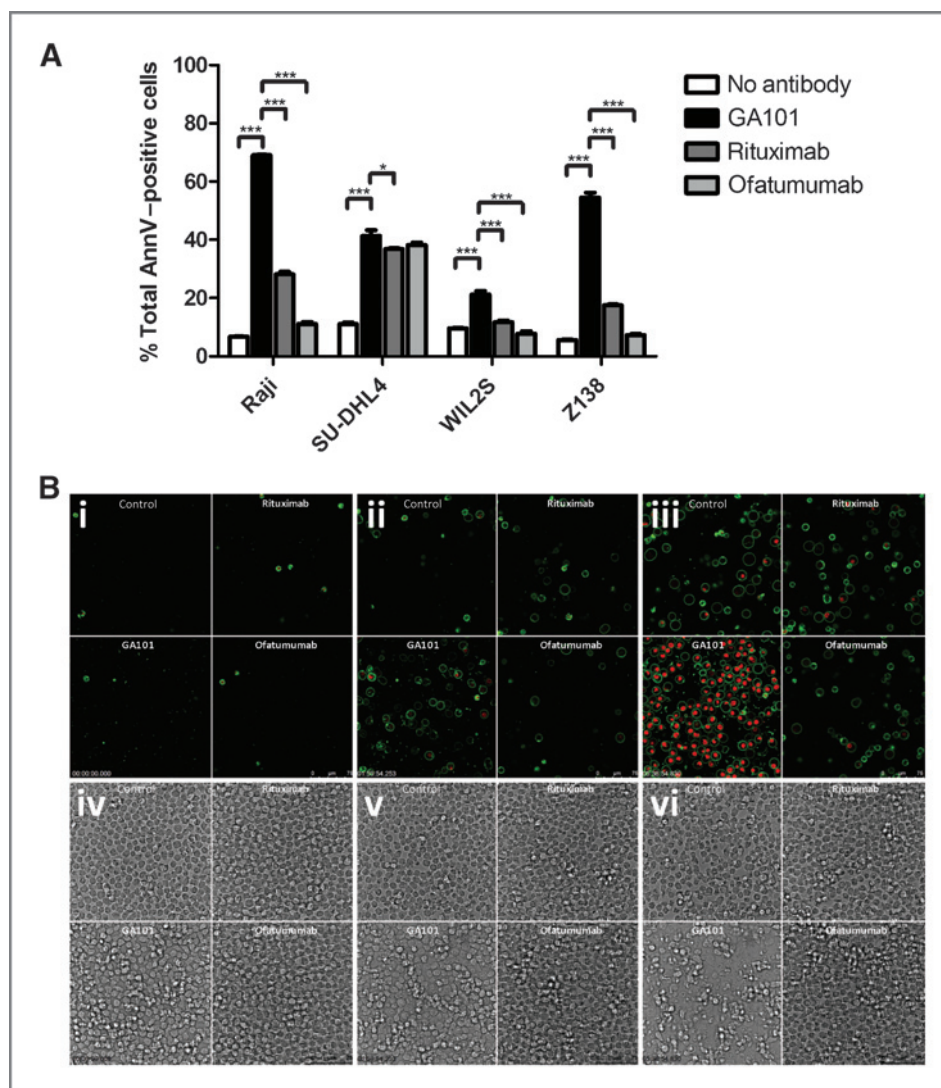
Figure 3. A, GA101-, rituximab-, and ofatumumab-mediated direct cell death assessed in four CD20-expressing cell lines, Raji, SU-DHL4, Wil2S, and Z138. Cells were incubated for 24 hours with CD20 antibodies (10 µg/mL) and subsequently stained with Annexin V–FITC and PI to detect apoptotic cells by flow cytometry. In three of four cell lines tested (Raji, Wil2S, and Z138), GA101 induced significantly stronger Annexin V^+/PI^+ cells compared with rituximab and ofatumumab. The data from one of three independent experiments carried out for each cell line are shown. The average and SDs were calculated from the triplicates in each experiment. Statistical analysis, Student t test, ***, $P < 0.0001$; *, $P \leq 0.05$. B, time-lapse imaging of direct cell-death induction in Z138 lymphoma cells treated with rituximab, ofatumumab, or GA101. Images were taken at time = 0 (i and iv), time = 2 hours (ii and v), and time = 5.5 hours (iii and vi). Fluorescent (i)–(iii) represent Annexin V (Ann V) FLUOS (detects phosphatidylserine exposure, green) and PI (detects loss of membrane integrity, red). Corresponding transmission images are shown in (iv)–(vi). Control- (buffer only), rituximab-, and ofatumumab-treated cells display limited direct cell-death induction. In contrast, incubation with GA101 leads to profound cell death within 5 to 6 hours. See also Supplementary Video S1.

GA101 vs. ~40 ng/mL for rituximab and ofatumumab on Z138 cells; ~0.3 ng/mL for GA101 vs. ~5–7 ng/mL for rituximab and ofatumumab on SU-DHL4 cells) and higher overall killing efficacy, particularly at low antibody concentrations. Notably, this was maintained even at high antibody concentrations (Fig. 4E). Non-glycoengineered GA101 (GA101 WT) displayed comparable ADCC activity to rituximab and ofatumumab confirming that glycoengineering (and therefore the enhanced affinity to FcγRIIIa), rather than type I versus type II binding mode, is the predominant factor conferring superior ADCC activity. Therefore, despite occupying only half the number of CD20 receptor-binding sites, GA101 achieves superior ADCC compared with rituximab and ofatumumab bearing a WT Fc portion.

ADCP

The ADCP-mediating activity of the three antibodies was compared using M1 and M2c macrophages generated from human MDMs (Fig. 4F). PKH26-labeled Raji cells were incubated for 1 hour with M1 or M2c in the presence of increasing concentrations of GA101, rituximab, and ofatumumab. ADCP was determined by FACS analysis. Overall, M2c macrophages displayed superior phagocytic activity compared with M1 macrophages at all antibody concentrations tested (Fig. 4F). No significant differences were observed between the three antibodies with respect to ADCP (Fig. 4F). The ADCP activity was further assessed in presence of physiologic concentrations of competing endogenous human IgGs (10 mg/mL), a condition that more closely resembles the natural setting (Fig. 4G). As before, GA101, rituximab, and ofatumumab displayed comparable phagocytic activity.

Internalization of antibody-bound CD20

The internalization of GA101, rituximab, and ofatumumab was determined by FACS analysis after incubation of SU-DHL4 cells (Supplementary Fig. S1A) and human
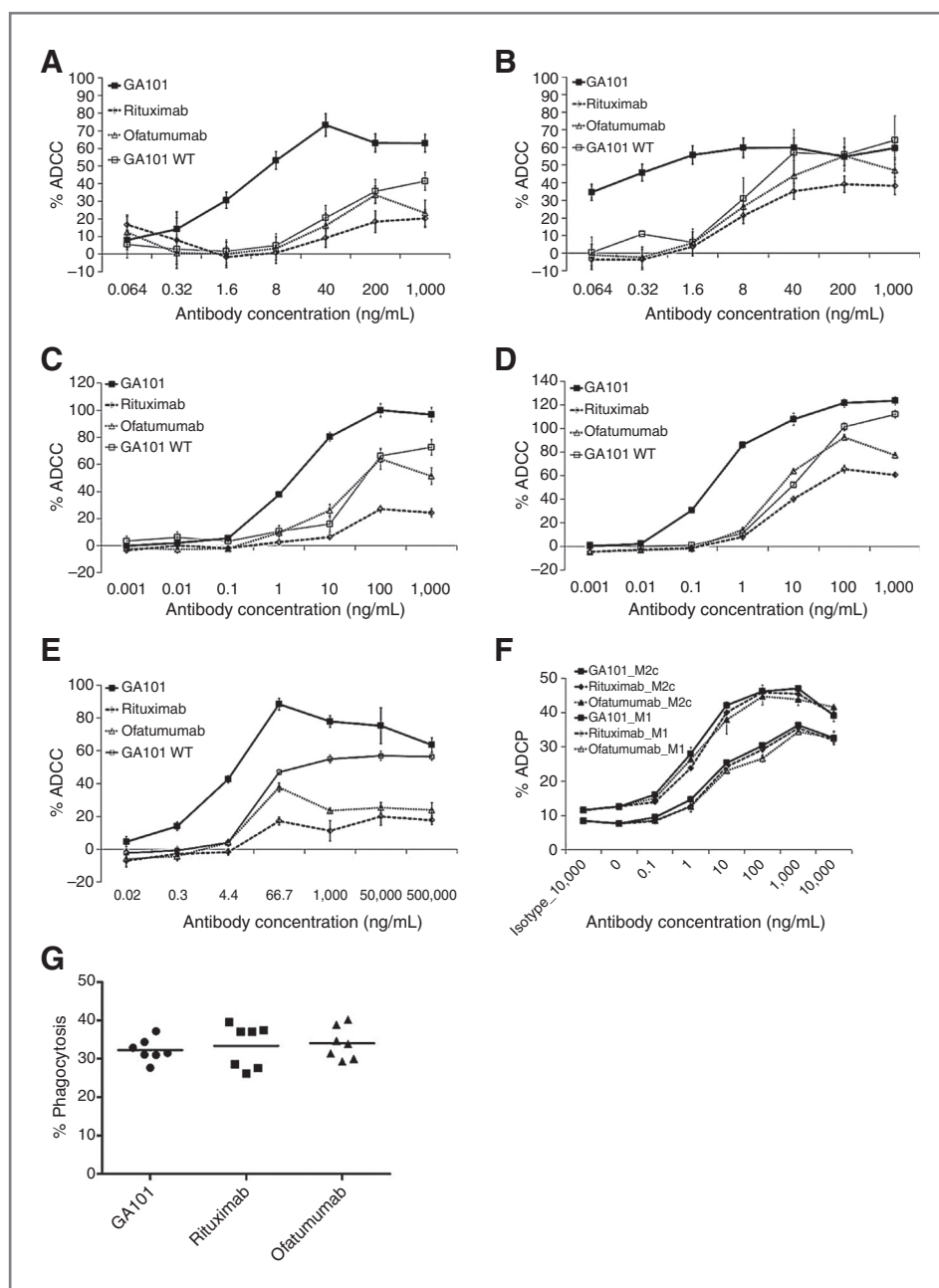
Figure 4. ADCC induced by standard doses of GA101 (black squares), GA101 WT (open squares), rituximab (open diamonds), and ofatumumab (open triangles). Cells were incubated for 4 hours in the presence of the CD20 antibodies and human PBMCs as effectors (E:T, 25:1) and percentage of ADCC was calculated by measuring lactate dehydrogenase release in cell supernatants. PBMCs expressing the V158/V158 FcγRIIIa receptor were incubated with Z138 (A) and SU-DHL4 (B) cell lines. PBMCs expressing the F158/F158 FcγRIIIa receptor were incubated with Z138 (C) and SU-DHL4 (D) cell lines. High doses of GA101 (black squares), GA101 WT (open squares), rituximab (open diamonds), and ofatumumab (open triangles) were added to Z138 cell lines incubated in the presence of PBMCs expressing the V158/V158 FcγRIIIa receptor (E). GA101 induces higher levels of ADCC compared with rituximab and ofatumumab even at high antibody concentrations. The average and SDs were calculated from the triplicates of each experiment. The data from one of three independent experiments are shown. Calculated EC$_{50}$ values: (A): GA101, 16 pmol/L; rituximab, 269 pmol/L; ofatumumab, approximately 262 pmol/L; GA101 WT, 302 pmol/L; (B): GA101, <2 pmol/L; rituximab, 38.7 pmol/L; ofatumumab, 47.3 pmol/L; GA101 WT, 57.3 pmol/L; (C): GA101, 12 pmol/L; rituximab, approximately 78 pmol/L; ofatumumab, approximately 69.3 pmol/L; GA101 WT, 182.7 pmol/L; (D): GA101, 2 pmol/L; rituximab, approximately 35 pmol/L; ofatumumab, approximately 23 pmol/L; GA101 WT, 79.3 pmol/L; (E): GA101, approximately 30 pmol/L; rituximab, approximately 39 pmol/L; ofatumumab, approximately 36 pmol/L; GA101 WT, 140 pmol/L. F, ADCP of Raji cells by human MDMs polarized to M1 or M2c subtypes. Raji cells were incubated with M1 or M2c macrophages for 1 hour (E:T, 3:1) in the presence of increasing concentrations of the CD20 antibodies. Analysis of phagocytosed target cells, assessed by flow cytometry, showed that all three antibodies induced comparable levels of ADCP. M2c displayed superior phagocytic activity compared with M1 macrophages. Calculated EC$_{50}$ values: M1: GA101, 28 pmol/L; rituximab, 32.7 pmol/L; ofatumumab, 38 pmol/L; M2c: GA101, 8 pmol/L; rituximab, 11.3 pmol/L; ofatumumab, 8 pmol/L. G, ADCP of Raji cells by human M2c macrophages (E:T, 3:1) in presence of 10 mg/mL competing human IgG (Redimune) and 1 μg/mL CD20 antibodies for 4 hours. Analysis of phagocytosed target cells, assessed by flow cytometry, showed that all three antibodies induced comparable levels of ADCP in presence of competing human IgGs.

blood derived from 2 patients with CLL (Supplementary Fig. S1B and S1C) with fluorescently labeled antibodies. Increased stability of surface-accessible CD20 was observed after GA101 treatment compared with ofatumumab and rituximab using both *in vitro* cultured cell line and primary CLL samples (Supplementary Fig. S1A–S1C). GA101 persisted longer on cell surface and thus displayed lower degree of internalization in comparison with rituximab and ofatumumab [the decrease in percentage of the surface accessible CD20 between 5 hours and 30 minutes of internalization was 2.5% for GA101 compared with 43% and 27% for rituximab and ofatumumab using primary CLL samples; 8% for GA101 compared with 18% and 22% for rituximab and ofatumumab using SU-DHL4 cells (measured between 7 hours and 30 minutes of internalization)]. These data indicate that GA101 persists slightly longer on the surface of tumor cells than do rituximab and ofatumumab and confirm that ofatumumab reduces the amount of surface-accessible CD20 in accordance with previously published findings with patient-derived NHL cells (15).

Whole-blood B-cell depletion

The activity of the antibodies was further compared in whole-blood B-cell depletion assays, which integrate different antibody modes of action (CDC, ADCC, and induction of cell death). Heparinized blood samples from healthy volunteers, representing each of the three FcγRIIIa genotypes [high-affinity (158V/158V), intermediate-affinity (158F/158V), and low-affinity (158F/158F) receptors], were examined. GA101 displayed the highest capacity of B-cell depletion regardless of the FcγRIIIa genotype and antibody concentrations used (Fig. 5A–C). The superiority

of GA101 compared with rituximab and ofatumumab is shown both by lower EC_{50} values and by higher maximal B-cell depletion (Supplementary Table S1). Interestingly, rituximab and ofatumumab induced B-cell depletion at antibody concentrations ≤50 ng/mL (with ofatumumab being superior to rituximab), but at concentrations higher than 50 ng/mL the B-cell depletion properties of ofatumumab declined. The phenomenon was more evident at very high antibody concentrations (up to 500 ng/mL; Fig. 5; Supplementary Fig. S2) at which ofatumumab almost completely lost its efficacy, whereas the activity of GA101 and rituximab was maintained. To exclude the possibility that heparin-mediated complement inhibition underlies the superiority of GA101 compared with rituximab and ofatumumab, B-cell depletion was assessed in whole-blood samples treated with lepirudin, a thrombin-specific agent that does not interfere with complement activation (Supplementary Fig. S2A and S2B). GA101 was superior to rituximab and ofatumumab in both heparin- and lepirudin-treated whole-blood samples, confirming that the mechanisms underlying GA101's superior B-cell depletion are complement-independent.

To further confirm the above-mentioned findings, B-cell depletion was assessed in autologous normal and heat-inactivated blood samples. Overall, heat inactivation of plasma samples reduced the B-cell depletion capacity of all antibodies (Supplementary Fig. S2C). Rituximab and ofatumumab efficacy was strongly affected by heat inactivation, leading to a drop in maximal B-cell depletion from 45% to 50% in normal blood to less than 10% in heat-inactivated blood (Supplementary Fig. S2C). Taken together, the experiments confirmed that ofatumumab and rituximab more strongly rely on CDC for efficient
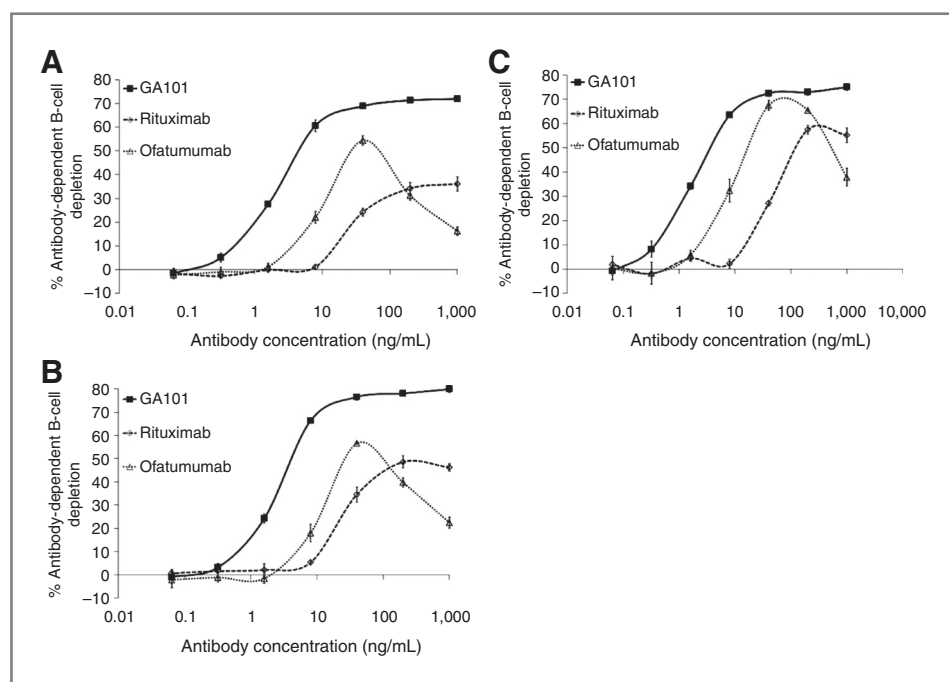

Figure 5. Whole-blood B-cell depletion mediated by GA101 (black squares), rituximab (open diamonds), and ofatumumab (open triangles) in heparin-treated whole-blood samples: F/F donor (A), F/V donor (B), V/V donor (C). The average B-cell depletion and SDs were calculated from the triplicates of each experiment. The data from one of three independent experiments for each genotype are shown. Average values of triplicates corresponding to EC_{50} values, percentage maximal killing and statistical analysis conducted for each donor and genotypes (3 donors/genotype, total of 9 experiments) are included in the Supplementary Table S1.

B-cell depletion. GA101 activity was only marginally affected by heat inactivation (B-cell depletion declined from 60% to 40%), allowing it to maintain superior activity under all assay conditions.

Antitumor activity in an SU-DHL4 and RL xenograft model

We have previously shown that GA101 mediates dose-dependent efficacy in the SU-DHL4 NHL xenograft model in SCID beige mice, with complete tumor remission observed with GA101 at doses of 30 mg/kg (1). In contrast, the efficacy of the type I CD20 antibody, rituximab, cannot be further enhanced by increasing doses. Here, we compared the single-agent efficacy of the three antibodies at 30 mg/kg doses in mice bearing large established subcutaneous SU-DHL4 tumors. Assessment of the first-line TGI on day 46 after tumor-cell inoculation showed tumor regression with GA101 (TGI, 120%) but only tumor stasis with rituximab and ofatumumab (100% or 106%, respectively) compared with the control group (Fig. 6A). Furthermore, at day 67, 7 of 10 mice in the GA101 group were tumor-free compared with only 4 of 10 and 2 of 10 mice in the rituximab or ofatumumab groups, respectively. For the assessment of second-line antitumor activity, mice bearing large established subcutaneous SU-DHL4 tumors first received two once-weekly doses of rituximab (10 mg/kg, i.p.) starting on day 25 after tumor inoculation before administration of GA101, rituximab, ofatumumab,

or vehicle control on day 39. Second-line treatment with GA101, rituximab, and ofatumumab resulted in a TGI of 64%, 20%, and 26%, respectively, on day 64 compared with control (Fig. 6B), with one animal from the GA101 group achieving complete remission at day 63. These data indicate that only treatment with GA101 resulted in a significantly increased TGI compared with control in the presence of residual amounts of rituximab. We have previously shown a superior antitumor efficacy of GA101 in the RL follicular NHL xenograft model as compared with rituximab (16). In the current study, we compared the single-agent efficacy of GA101, rituximab, and of atumumab at a dose of 30 mg/kg. Treatment was initiated on day 14 after tumor inoculation in mice bearing established subcutaneous RL tumors with a median volume of 150 mm^3. Treatment with rituximab, ofatumumab, or GA101 resulted in a statistically significant TGI compared with control of 57%, 59%, or 82%, respectively, on day 28 (Fig. 6C).

Discussion

The introduction of rituximab into clinical practice has markedly advanced the treatment of hematologic malignancies (17–19). The success of CD20 as a target for treatment led to development of other CD20 antibodies in efforts to further improve patient outcome and provide treatment options for individuals refractory to rituximab including GA101, a glycoengineered type II antibody and
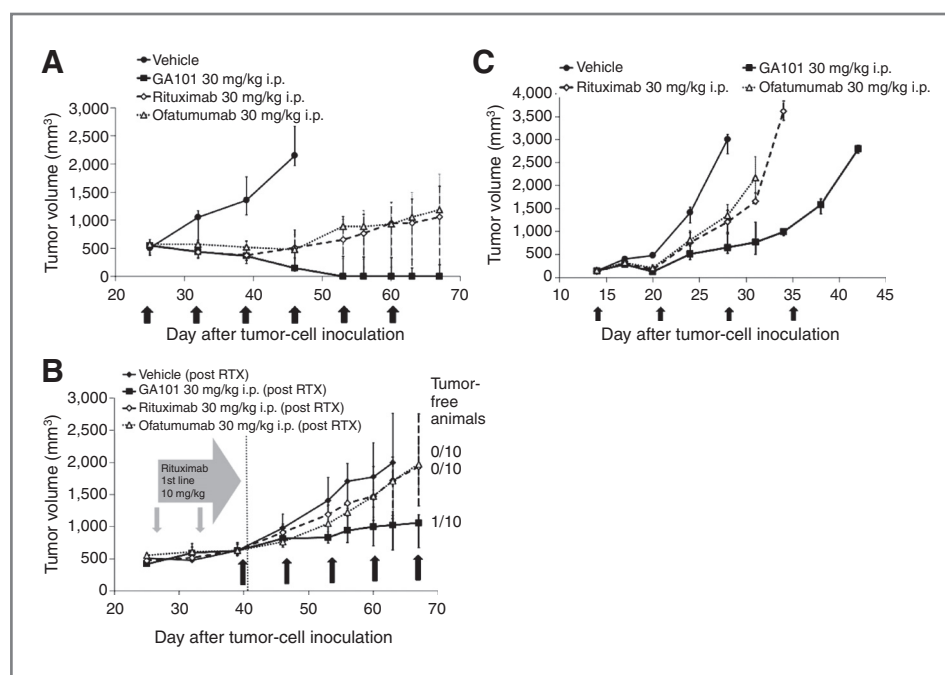

Figure 6. A, antitumor activity of GA101 (black squares), rituximab (open diamonds), and ofatumumab (open triangles) in a subcutaneous SU-DHL4 model (six once-weekly 30 mg/kg, i.p. doses commencing on day 25 after tumor inoculation; median and interquartile range; $n = 10$ animals/group). B, antitumor activity of GA101, rituximab, and ofatumumab (five once-weekly 30 mg/kg, i.p. doses) given as second-line treatment following first-line rituximab therapy (two once-weekly doses of 10 mg/kg, i.p. starting on day 25 after tumor inoculation; median and interquartile range; $n = 7–9$ animals/group). C, antitumor activity of GA101, rituximab, and ofatumumab (30 mg/kg, i.p. once-weekly) in subcutaneous RL model (median and interquartile range; $n = 10$ animals/group). In the rituximab and ofatumumab groups, mice received an injection on days 14, 21, and 28. In the GA101 group, mice received an injection on days 14, 21, 28, and 35.

the type I antibody ofatumumab. The current study compared the activity of the three CD20 antibodies in a broad panel of *in vitro* assays, including binding to target cells, induction of direct cell death, CDC, ADCC, and whole-blood B-cell depletion. The antitumor activities were further compared in xenograft tumor models *in vivo*.

Overall, GA101 showed a different activity profile from both type I antibodies, rituximab and ofatumumab. Despite displaying only half of the maximal binding to CD20, GA101 induced higher levels of direct cell death than rituximab or ofatumumab in a panel of CD20-expressing tumor cell lines as well as higher ADCC. It can be hypothesized that the 2:1 binding ratio may be due to different binding to CD20 tetramers: for example, intertetramer binding for rituximab and ofatumumab versus intratetramer binding for GA101. Superior direct effects of GA101 were confirmed using time-lapse video microscopy, which showed that cell death (detected by Annexin V expression and PI uptake) occurs rapidly following GA101 but only marginally following rituximab and ofatumumab binding. This is in line with published data showing lower degree of cell death by rituximab and ofatumumab than for GA101 (7). These findings further support the recent observations proposing a novel, lysosome-dependent induction of cell death by GA101 involving actin polymerization, release of cathepsins, and reactive oxygen species (6). They do not support the recently postulated conclusions that the enhanced induction of direct cell death attributed to GA101 and other antibodies (20, 21), may be a consequence of mechanical disruption during FACS analysis (13, 14).

As expected, GA101 was superior to rituximab and ofatumumab in ADCC, an activity conferred by glycoengineering and increased affinity for FcγRIIIa (CD16) on natural killer cells. Enhanced ADCC may be further strengthened by the lower induction of CD20 downmodulation observed upon binding of GA101 in comparison to rituximab and ofatumumab (3, 15), also confirmed in the current study.

GA101 was found to be inferior to both rituximab and ofatumumab in mediating CDC at low antibody concentrations *in vitro*. Notably, this difference was not as significant at higher antibody concentrations. Type I antibodies are believed to induce higher levels of CDC than type II antibodies owing to stronger binding of type I antibody/CD20 complexes within lipid rafts to C1q, the first subcomponent of classical complement activation (22, 23). Unlike type I antibodies, GA101 does not cluster CD20 molecules into lipid rafts on surface of B cells (1), which may explain its lower CDC induction seen *in vitro* at low antibody concentrations (≤10 µg/mL). However, in clinical practice, the CD20 antibodies are dosed at high concentrations resulting in trough levels >10 µg/mL. It is therefore possible that differences in CDC between type I and II antibodies observed *in vitro* may not be present in the clinical setting.

Rituximab and ofatumumab were found to have comparable CDC and ADCC activity using two NHL cell lines,

Z138 and SU-DHL4, representing low and high CD20 expression levels, respectively. These findings are in contrast to previous reports where ofatumumab was shown to be more efficacious than rituximab (10, 24, 25). It has been postulated that by binding to both the small and the large loop of CD20, ofatumumab may bind to CD20 in a more membrane-proximal manner than does rituximab (10, 12, 26). Although the membrane proximity argument may be valid for large membrane proteins such as melanoma chondroitin sulfate proteoglycan (MCSP; ref. 27), it may not necessarily apply to membrane proteins with small extracellular domains such as CD20. It is difficult to argue why in our assays the described hallmark of ofatumumab, namely the improved CDC, is not enhanced compared with rituximab using NHL cell lines. Indeed, Teeling and colleagues (26) did not show enhanced CDC for all three cell lines that were investigated and other publications show comparable CDC between ofatumumab and rituximab on a number of cell lines (28, 29). Therefore, enhanced CDC cannot be considered as general property of ofatumumab but may be observed under certain, more sensitive conditions, for example, when using CLL samples (30, 31). These data are in line with Rafiq and colleagues (31) who showed that GA101 mediated superior cell-death induction and ADCC, but reduced CDC as compared with rituximab and ofatumumab in primary CLL samples. However, differently from Rafiq and colleagues' observations (31), we found that GA101, rituximab, and ofatumumab mediate comparable ADCP when using NHL cell lines and primary human MDMs.

In whole-blood B-cell deletion assays, which integrate different antibody activities (CDC, ADCC, and induction of cell death) and thus may more accurately reproduce the clinical setting, GA101 was superior to both rituximab and ofatumumab. In addition, experiments carried out using heat-inactivated serum confirmed that CDC plays a more important role for B-cell depletion of type I than of type II CD20 antibodies. We observed that ofatumumab was clearly superior to rituximab at low antibody concentrations, whereas at higher concentrations (>50 ng/mL) its B-cell depletion properties declined. It is thought that both ofatumumab and rituximab mediate tumor cell killing via ADCC until saturation and that at higher concentrations complement fixation occurs, which may interfere with ADCC resulting in a "bell-shaped" curve (32, 33). Therefore, the decreased B-cell depletion observed with ofatumumab at high antibody concentrations may be attributable to the reported increased affinity of ofatumumab for complement factors (10), although in the current study, we did not detect any significant difference in complement binding and CDC activity *in vitro*. A recent study by Beurskens and colleagues implies that maximal B-cell killing with ofatumumab and rituximab *in vitro* is indeed achieved with intermediate antibody concentrations, whereas lower overall killing is achieved using higher antibody concentrations, an effect attributed to effector cell exhaustion (34). Taken together, our data show that B-cell depletion by GA101 is superior to both

rituximab and ofatumumab, under conditions where CDC is retained. The superior activity of GA101 in whole-blood assays may thus be attributable to its higher FcγRIIIa affinity, ADCC, and induction of direct cell death. Two studies have recently shown the important contribution of ADCC to overall killing in whole-blood B-cell depletion assays using patients with CLL (35, 36). *In vivo* B-cell depletion studies in cynomolgus monkeys support that superior B-cell depletion translates to the *in vivo* setting (1).

Notably, our data provide the first direct *in vivo* comparison of the three CD20 antibodies, GA101, rituximab, and ofatumumab in established xenografts models. The 30 mg/kg weekly dose was selected on the basis of previous studies that showed that dose increments from 10 to 30 mg/kg led to complete tumor remission with GA101 but not rituximab in the subcutaneous SU-DHL4 xenograft model (1). Importantly, trough levels achieved with a weekly dose of 30 mg/kg in mice are in the 300 to 400 μg/mL range, matching the clinical trough levels of dose-dense rituximab and GA101 schedules in clinical trials (data not shown; refs. 37, 38). *In vivo* studies comparing GA101 and its non-glycoengineered version in the SU-DHL4 model showed comparable antitumoral efficacy and tumor remission for both antibodies indicating that the superior activity of GA101 is not related to glycoengineering, but rather to direct effects. Nevertheless, a contribution of macrophages to the overall mode of action is possible. In contrast to Barth and colleagues (39) who showed superiority of ofatumumab over rituximab in a rituximab-resistant model, we observed comparable efficacy for the two type I antibodies. It may be possible that ofatumumab shows superior antitumor efficacy in xenograft models based on rituximab-resistant cell lines, whereas it shows equal efficacy in conventional models. However, to date, the molecular mechanisms for rituximab resistance (other than CD20 loss) have not been fully understood and are subject of on-going research. Taken together, the preclinical *in vivo* experiments show that GA101 can induce tumor remission and tumor stasis in a second-line setting, whereas rituximab, as well as ofatumumab, can neither induce remission of large established subcutaneous SU-DHL4 tumors nor control tumor progression under rituximab therapy.

In summary, our preclinical data show that the glycoenginereed type II CD20 antibody GA101 (obinutuzumab) is differentiated from the two approved type I CD20 antibodies, rituximab and ofatumumab, by its superior overall *in vitro* and *in vivo* activity supporting its further clinical investigation. In contrast to previous reports (40), we were not able to show superior activity of ofatumumab compared with rituximab *in vitro* or *in vivo*. Ultimately, large randomized head-to-head clinical studies comparing these antibodies will be required to show whether the preclinical findings reflect the clinical efficacy of CD20 antibodies controlling NHL and CLL.

References

1. Mossner E, Brunker P, Moser S, Puntener U, Schmidt C, Herter S, et al. Increasing the efficacy of CD20 antibody therapy through the engineering of a new type II anti-CD20 antibody with enhanced direct and immune effector cell-mediated B-cell cytotoxicity. Blood 2010;115:4393–402.
2. Ferrara C, Grau S, Jager C, Sondermann P, Brunker P, Waldhauer I, et al. Unique carbohydrate-carbohydrate interactions are required for high affinity binding between FcgammaRIII and antibodies lacking core fucose. Proc Natl Acad Sci U S A 2011;108:12669–74.
3. Beers SA, French RR, Chan HT, Lim SH, Jarrett TC, Vidal RM, et al. Antigenic modulation limits the efficacy of anti-CD20 antibodies: implications for antibody selection. Blood 2010;115:5191–201.
4. Ivanov A, Beers SA, Walshe CA, Honeychurch J, Alduaij W, Cox KL, et al. Monoclonal antibodies directed to CD20 and HLA-DR can elicit homotypic adhesion followed by lysosome-mediated cell death in human lymphoma and leukemia cells. J Clin Invest 2009;119:2143–59.
5. Niederfellner G, Lammens A, Mundigl O, Georges GJ, Schaefer W, Schwaiger M, et al. Epitope characterization and crystal structure of GA101 provide insights into the molecular basis for type I/II distinction of CD20 antibodies. Blood 2011;118:358–67.
6. Alduaij W, Ivanov A, Honeychurch J, Cheadle EJ, Potluri S, Lim SH, et al. Novel type II anti-CD20 monoclonal antibody (GA101) evokes

homotypic adhesion and actin-dependent, lysosome-mediated cell death in B-cell malignancies. Blood 2011;117:4519–24.

7. Honeychurch J, Alduaij W, Azizyan M, Cheadle EJ, Pelicano H, Ivanov A, et al. Antibody-induced nonapoptotic cell death in human lymphoma and leukemia cells is mediated through a novel reactive oxygen species-dependent pathway. Blood 2012;119:3523–33.

8. Gravanis I, Ersboll J, Skovlund E, Abadie E, Marty M, Pignatti F. The European Medicines Agency review of ofatumumab (Arzerra(R)) for the treatment of chronic lymphocytic leukemia in patients refractory to fludarabine and alemtuzumab: summary of the scientific assessment of the European medicines agency committee for medicinal products for human use. Oncologist 2010;15:1335–43.

9. Lemery SJ, Zhang J, Rothmann MD, Yang J, Earp J, Zhao H, et al. U.S. Food and Drug Administration approval: ofatumumab for the treatment of patients with chronic lymphocytic leukemia refractory to fludarabine and alemtuzumab. Clin Cancer Res 2010;16:4331–8.

10. Pawluczkowycz AW, Beurskens FJ, Beum PV, Lindorfer MA, van de Winkel JG, Parren PW, et al. Binding of submaximal C1q promotes complement-dependent cytotoxicity (CDC) of B cells opsonized with anti-CD20 mAbs ofatumumab (OFA) or rituximab (RTX): considerably higher levels of CDC are induced by OFA than by RTX. J Immunol 2009;183:749–58.

11. Engelberts J, Beurskens F, Mackus W, Bakker J, Vink T, Tiebout A, et al. Ofatumumab targets a conformational membrane-proximal epitope which contains amino acids located in the small and large loops of CD20. Haematol-Hematol J 2010;95:46-.

12. Teeling JL, Mackus WJ, Wiegman LJ, van den Brakel JH, Beers SA, French RR, et al. The biological activity of human CD20 monoclonal antibodies is linked to unique epitopes on CD20. J Immunol 2006;177: 362–71.

13. Golay J, Bologna L, Andre PA, Buchegger F, Mach JP, Boumsell L, et al. Possible misinterpretation of the mode of action of therapeutic antibodies in vitro: homotypic adhesion and flow cytometry result in artefactual direct cell death. Blood 2010;116:3372–3.

14. Cragg MS, Alduaij W, Klein C, Umana P, Glennie MJ, Illidge TM. Novel lysosomal-dependent cell death following homotypic adhesion occurs within cell aggregates Response. Blood 2010;116:3373–4.

15. Lim SH, Vaughan AT, Ashton-Key M, Williams EL, Dixon SV, Chan HT, et al. Fc gamma receptor IIb on target B cells promotes rituximab internalization and reduces clinical efficacy. Blood 2011;118: 2530–40.

16. Dalle S, Reslan L, Besseyre de Horts T, Herveau S, Herting F, Plesa A, et al. Preclinical studies on the mechanism of action and the anti-lymphoma activity of the novel anti-CD20 antibody GA101. Mol Cancer Ther 2011;10:178–85.

17. Marcus R, Imrie K, Solal-Celigny P, Catalano JV, Dmoszynska A, Raposo JC, et al. Phase III study of R-CVP compared with cyclophosphamide, vincristine, and prednisone alone in patients with previously untreated advanced follicular lymphoma. J Clin Oncol 2008;26: 4579–86.

18. Coiffier B, Thieblemont C, Van Den Neste E, Lepeu G, Plantier I, Castaigne S, et al. Long-term outcome of patients in the LNH-98.5 trial, the first randomized study comparing rituximab-CHOP to standard CHOP chemotherapy in DLBCL patients: a study by the Groupe d'Etudes des Lymphomes de l'Adulte. Blood 2010;116:2040–5.

19. Hallek M, Fischer K, Fingerle-Rowson G, Fink AM, Busch R, Mayer J, et al. Addition of rituximab to fludarabine and cyclophosphamide in patients with chronic lymphocytic leukaemia: a randomised, open-label, phase 3 trial. Lancet 2010;376:1164–74.

20. Krause G, Patz M, Isaeva P, Wigger M, Baki I, Vondey V, et al. Action of novel CD37 antibodies on chronic lymphocytic leukemia cells. Leukemia 2012;26:546–9.

21. Heider KH, Kiefer K, Zenz T, Volden M, Stilgenbauer S, Ostermann E, et al. A novel Fc-engineered monoclonal antibody to CD37 with enhanced ADCC and high proapoptotic activity for treatment of B-cell malignancies. Blood 2011;118:4159–68.

22. Cragg MS, Glennie MJ. Antibody specificity controls in vivo effector mechanisms of anti-CD20 reagents. Blood 2004;103:2738–43.

23. Kishore U, Reid KB. C1q: structure, function, and receptors. Immunopharmacology 2000;49:159–70.

24. Taylor RP, Pawluczkowycz AW, Beum PV, Lindorfer MA, Beurskens F, van de Winkel J, et al. Complement activation and comlement-mediated killing of B cells promoted by anti-CD20 monoclonal antibodies (mAb) rituximab and ofatumumab are rapid, and ofatumumab kills cells more rapidly and with greater efficacy. Blood 2007;110:695a-a.

25. Beurskens J, Mackus W, Engelberts P, Miller S, Speller S, Chamberlain L, et al. NK cell binding and induction of potent NK cell-mediated ADCC by ofatumumab, a new human CD20 monoclonal antibody [abstract]. Haematologica 2010;95(Suppl 2):173. Abstract nr 0426.

26. Teeling JL, French RR, Cragg MS, van den Brakel J, Pluyter M, Huang H, et al. Characterization of new human CD20 monoclonal antibodies with potent cytolytic activity against non-Hodgkin lymphomas. Blood 2004;104:1793–800.

27. Bluemel C, Hausmann S, Fluhr P, Sriskandarajah M, Stallcup WB, Baeuerle PA, et al. Epitope distance to the target cell membrane and antigen size determine the potency of T cell-mediated lysis by BiTE antibodies specific for a large melanoma surface antigen. Cancer Immunol Immunother 2010;59:1197–209.

28. Nishida M, Teshigawara K, Niwa O, Usuda S, Nakamura T, Ralph P, et al. Novel humanized anti-CD20 monoclonal antibodies with unique germline VH and VL gene recruitment and potent effector functions. Int J Oncol 2008;32:1263–74.

29. Uchiyama S, Suzuki Y, Otake K, Yokoyama M, Ohta M, Aikawa S, et al. Development of novel humanized anti-CD20 antibodies based on affinity constant and epitope. Cancer Sci 2010;101:201–9.

30. Bologna L, Gotti E, Da Roit F, Intermesoli T, Rambaldi A, Introna M, et al. Ofatumumab is more efficient than rituximab in lysing B chronic lymphocytic leukemia cells in whole blood and in combination with chemotherapy. J Immunol 2013;190:231–9.

31. Rafiq S, Butchar JP, Cheney C, Mo X, Trotta R, Caligiuri M, et al. Comparative assessment of clinically utilized CD20-directed antibodies in chronic lymphocytic leukemia cells reveals divergent NK cell, monocyte, and macrophage properties. J Immunol 2013;190:2702–11.

32. Wang SY, Racila E, Taylor RP, Weiner GJ. NK-cell activation and antibody-dependent cellular cytotoxicity induced by rituximab-coated target cells is inhibited by the C3b component of complement. Blood 2008;111:1456–63.

33. Kern DJ, James BR, Blackwell S, Gassner C, Klein C, Weiner GJ. GA101 induces NK-cell activation and antibody-dependent cellular cytotoxicity more effectively than rituximab when complement is present. Leuk Lymphoma. Epub 2013 Apr 16.

34. Beurskens FJ, Lindorfer MA, Farooqui M, Beum PV, Engelberts P, Mackus WJ, et al. Exhaustion of cytotoxic effector systems may limit monoclonal antibody-based immunotherapy in cancer patients. J Immunol 2012;188:3532–41.

35. Patz M, Isaeva P, Forcob N, Muller B, Frenzel LP, Wendtner CM, et al. Comparison of the in vitro effects of the anti-CD20 antibodies rituximab and GA101 on chronic lymphocytic leukaemia cells. Br J Haematol 2011;152:295–306.

36. Bologna L, Gotti E, Manganini M, Rambaldi A, Intermesoli T, Introna M, et al. Mechanism of action of type II, glycoengineered, anti-CD20 monoclonal antibody GA101 in B-chronic lymphocytic leukemia whole blood assays in comparison with rituximab and alemtuzumab. J Immunol 2011;186:3762–9.

37. Sehn LH, Assouline SE, Stewart DA, Mangel J, Gascoyne RD, Fine G, et al. A phase 1 study of obinutuzumab induction followed by 2 years of maintenance in patients with relapsed CD20-positive B-cell malignancies. Blood 2012;119:5118–25.

38. Salles G, Morschhauser F, Lamy T, Milpied N, Thieblemont C, Tilly H, et al. Phase 1 study results of the type II glycoengineered humanized anti-CD20 monoclonal antibody obinutuzumab (GA101) in B-cell lymphoma patients. Blood 2012;119:5126–32.

39. Barth MJ, Hernandez-Ilizaliturri FJ, Mavis C, Tsai PC, Gibbs JF, Deeb G, et al. Ofatumumab demonstrates activity against rituximab-sensitive and -resistant cell lines, lymphoma xenografts and primary tumour cells from patients with B-cell lymphoma. Br J Haematol 2012;156:490–8.

40. Boross P, Jansen JH, de Haij S, Beurskens FJ, van der Poel CE, Bevaart L, et al. The in vivo mechanism of action of CD20 monoclonal antibodies depends on local tumor burden. Haematologica 2011;96: 1822–30.

Molecular Cancer Therapeutics

Preclinical Activity of the Type II CD20 Antibody GA101 (Obinutuzumab) Compared with Rituximab and Ofatumumab *In Vitro* and in Xenograft Models

Sylvia Herter, Frank Herting, Olaf Mundigl, et al.

Updated version	Access the most recent version of this article at: doi:10.1158/1535-7163.MCT-12-1182
Supplementary Material	Access the most recent supplemental material at: http://mct.aacrjournals.org/content/suppl/2013/07/22/1535-7163.MCT-12-1182.DC1

Cited articles	This article cites 38 articles, 27 of which you can access for free at: http://mct.aacrjournals.org/content/12/10/2031.full#ref-list-1
Citing articles	This article has been cited by 19 HighWire-hosted articles. Access the articles at: http://mct.aacrjournals.org/content/12/10/2031.full#related-urls

E-mail alerts	Sign up to receive free email-alerts related to this article or journal.
Reprints and Subscriptions	To order reprints of this article or to subscribe to the journal, contact the AACR Publications Department at pubs@aacr.org.
Permissions	To request permission to re-use all or part of this article, use this link http://mct.aacrjournals.org/content/12/10/2031. Click on "Request Permissions" which will take you to the Copyright Clearance Center's (CCC) Rightslink site.